A New Method to Assess the Jetting Behavior of Drop-On-Demand Inkjet Fluids

Sungjune Jung, Stephen D Hoath, Graham D Martin and Ian M Hutchings, Institute for Manufacturing, University of Cambridge, UK

Abstract

We present a new experimental method to assess the jetting performance of fluids for use in drop-on-demand (DoD) inkjet printheads. The oblique collision of two continuous liquid jets leads to the formation of a thin oval liquid sheet bounded by a thicker rim which disintegrates into ligaments and droplets. Under certain conditions the flow structure exhibits a remarkably symmetrical 'fishbone' pattern composed of a regular succession of longitudinal ligaments and droplets. For a series of model elastic fluids containing polystyrene (PS) in diethyl phthalate (DEP), ejected from nozzles with an internal diameter of 0.85 mm, the shape of the fishbone pattern varies strongly with polymer concentration. The same fluids were used in a Xaar piezoelectric DoD print head to characterize their jetting performance in terms of the maximum ligament length, a crucial parameter in determining the printability of the fluid. There are close similarities between the ligament collapse behaviors in both experiments. Good correlation was found between the maximum included angle of the fishbone pattern and the maximum ligament length in the jetting experiments, which suggests that a test based on oblique impinging jets may be useful in the development of fluids for inkjet printing.

Introduction

Inkjet printing technology has been widely applied not only to conventional graphics printing but also as an industrial manufacturing process for radio frequency identification (RFID) tags, printed circuit boards (PCBs) and organic electronics such as plastic organic light emitting diodes (P-OLEDs) and organic thin-film transistors (OTFTs), as well as to the deposition of biological material [1-5]. For optimal performance in drop on demand (DoD) inkjet printing, the fluid should satisfy specific physical properties. In the case of Newtonian fluids which have now been used for more than 30 years, it has been proposed that Z, the inverse of the Ohnesorge number of the fluid (Z = 1/Oh) must lie in the range $1 < Z < 10$ for proper drop formation [6]. More recently, a printable range of $4 < Z < 14$ has been suggested by considering characteristics such as single droplet formability, positional accuracy and maximum allowable jetting frequency [7]. Inkjet printing with non-Newtonian fluids, which is essential for various industrial applications, is significantly affected by the presence of viscoelasticity in the ink as the droplet is formed and ejected in a highly extensional flow. Poor jetting behavior will occur above a certain degree of viscoelasticity, which typically arises from the presence of polymers; such fluids may form jets with very long tails, or the jet may even fail to detach from the nozzle. So far, few studies have been conducted on the printability of viscoelastic fluids. Tuladhar and Mackley studied the correlation between filament stretching and jetting performance, using a variant of a multipass rheometer [8]. Hoath et al. tested dilute polystyrene solutions with different molecular weights to explore the limitations of the polymer content in an inkjet fluid. [9].

The present work examines the formation and breakup of the fluid structure created by the oblique collision of two impinging viscoelastic jets. In order to evaluate the effect of varying molecular weights and concentrations of polymers on the fluid structure, we focus on a transient regime, the so-called 'fishbone' [10], which involves periodic breakup of the stream into transverse ligaments and droplets. The possibility is then explored that observation of this fishbone structure might be used to access rheological information which is relevant to jetting performance from a piezo inkjet printhead.

Experimental fluids

Solutions containing polystyrene (PS) in diethyl phthalate (DEP) were formulated to investigate the systematic effects of polymer concentration and molecular weight. The 99.5% purity DEP was purchased from Sigma-Aldrich and PS was obtained from BASF. Solutions of linear PS with average molecular weights of 110,000 g/mol (designated PS110) and 210,000 g/mol (PS210) were prepared in DEP with varying concentrations from 0.01 wt% to 1 wt%. The viscosities were measured with a Viscolite 700 vibrational viscometer (Hydramotion Ltd., UK). Surface tension was measured with a bubble tensiometer (SITA pro line t15) and was essentially the same for all the polymer concentrations.

PAV characterization

The piezoelectric axial vibrator (PAV) is a squeeze-flow rheometer apparatus to characterize the viscoelastic behavior of complex fluids [11]. The storage modulus (G') and the loss modulus (G'') of a non-Newtonian fluid are obtained from the response of the test fluid to compression between stainless steel plates at high frequency f (up to 4 kHz). The total modulus can be expressed as $G^* = (G'^2 + G''^2)^{1/2}$. The variation of G' and G'' with frequency for the 1 wt% PS110 solution has been presented elsewhere [9]. The degree of viscoelasticity of the test fluid was characterized by the ratio G'/G^* at f = 1 kHz, since this frequency relates to the frequency of droplet generation (with a period of ~ 1 ms) in the fishbone regime, as shown below.

Experimental apparatus

A schematic diagram of the apparatus is presented in Fig. 1. Fluid from the reservoir was pumped through flexible tubing via a flow meter into a splitter, and divided between two identical stainless steel hypodermic needles (with flat ends) with an internal diameter of 0.85 mm. The angle between the axes of the two needles was held constant at 78°, for which the fishbone pattern was best developed in pure DEP. The jet lengths, defined as the distances from the ends of the nozzles to the impact point, were 3.5 mm and 6.5 mm. This asymmetry in nozzle position was required to generate the flow instability needed for a symmetrical fishbone structure, which also required precise alignment of the needles. The rotor-based flow meter with an electronic pulse output was calibrated for each solution by measuring the frequency of the pulses and the fluid volume ejected from the needles over a set time. The jet velocity from the nozzles was varied by changing the speed of the pump, in order to observe the progression of the resulting fluid pattern from ~1.5 to 6 m/s. The corresponding ranges of Reynolds number (Re) and Weber number (We) were 70< Re < 700 and 30 < We < 600.

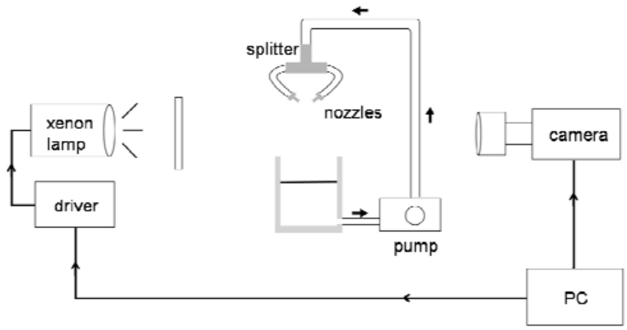

Figure 1. Experimental apparatus

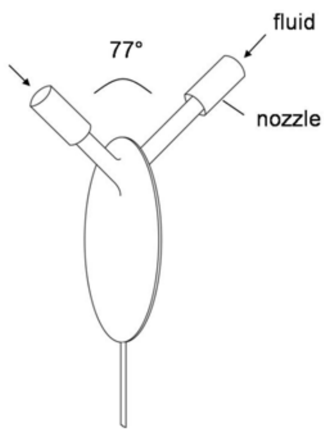

Figure 2. Schematic diagram showing the collision of two jets

Single-flash photography with back-illumination was used to capture individual images of the jet interaction region and to extract quantitative information such as the sizes of the resulting droplets and the spacing or angle between the droplet streams. The light source was a xenon lamp with ~1μs flash duration and the image was captured with a 10 megapixel digital single lens reflex camera (Nikon D40X). The short duration of the flash ensured that there was no significant motion blurring. The axis of the optical system was normal to the fluid sheet shown in Fig. 2.

In this experimental setup the lamp, camera and flow meter were controlled and synchronized by a PC data acquisition board (NI-6016, National Instruments) programmed with Labview. A digital pulse signal was sent from the NI-6016 to the remote controller of the camera, which operated with a 1/3 second shutter speed. Another pulse was produced with a specified delay time after the first one and transferred to the lamp controller, which generated a flash of light while the camera shutter was open. At the same time the board acquired a series of digital signals from the flow meter, so that the flow rate and hence jet velocity could be accurately recorded.

Observations

As seen in Fig. 3, the collision of two jets of a dilute solution of PS110 (0.02 wt% in DEP) with low viscoelasticity results in the formation of various fluid regimes with increasing flow velocity: oscillating streams (not shown); fluid chain (a); periodic atomization (the 'fishbone' form) (b); smooth single sheet (c); sheet with fluttering (d); disintegrating ruffled sheet (e); and violent flapping (f). Initially, the succession of sheets in the fluid chain in (a) consist of thin oval fluid regions each bounded by a thicker rim. The initial oval film becomes larger with a higher flow rate. Small perturbations on the rim start to appear and gradually grow, leading to periodic detachment of droplets. As the flow rate is increased, the pattern takes the characteristic fishbone form consisting of a fluid sheet, a series of ligaments and droplets. The ligaments elongate, and the degree of that extension depends on both the viscosity and elasticity of the fluid. When this pattern extends to its maximum length, it suddenly becomes converted into a stable single sheet larger than that seen in the fluid chain, and then on further increase in velocity becomes unstable again, giving rise to random droplets. As the jet velocity is increased further, the sheet becomes ruffled, forming a disintegrating ruffled sheet with a stable rim. Finally, violent flapping ensues at a very high flow rate.

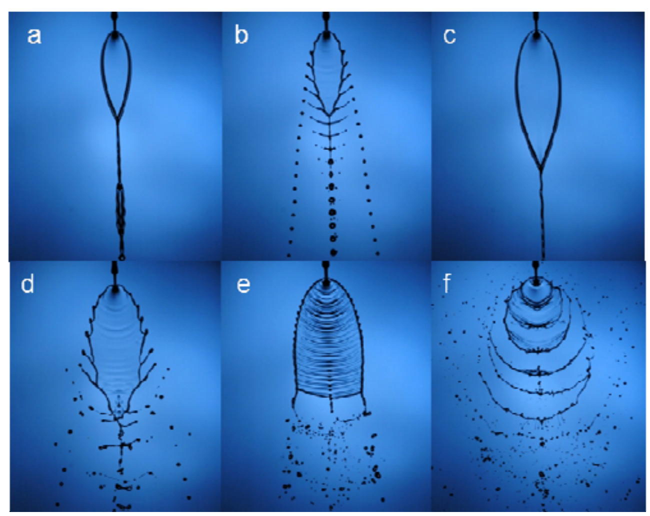

Figure 3. Single-flash images showing the evolution of the fluid sheets formed by impinging jets of a liquid with little viscoelasticity (0.02 wt% PS110 in DEP).

Image Processing

Image processing was performed in several steps as shown in Fig. 4. An 8-bit grayscale image (b) was obtained by extracting the intensity plane from an original HSI (Hue, Saturation and Intensity) image (a). In the next step, thresholding was applied to isolate objects of interest in the image. Through this process, the grayscale image with pixel values ranging from 0 to 255 was converted into a binary image with pixel values of 0 or 1 (c). Binary morphological operations were also performed in order to remove unwanted information. Finally, particle analysis was carried out to make measurements such as drop diameter, drop spacing and stream angle, defined by 4 points.

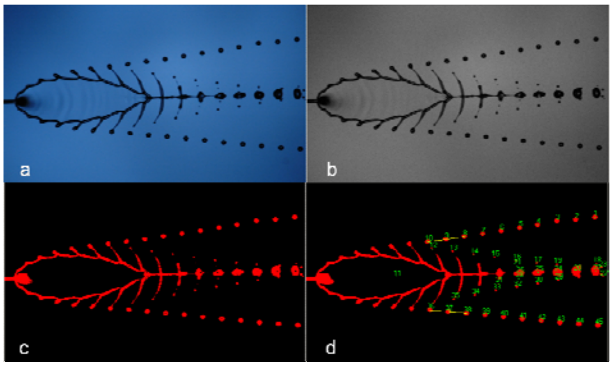

Figure 4. Image processing sequence. Images are rotated through 90°. 24-bit RGB (a), 8-bit grayscale (b), 2-bit binary (c), particle analysis (d)

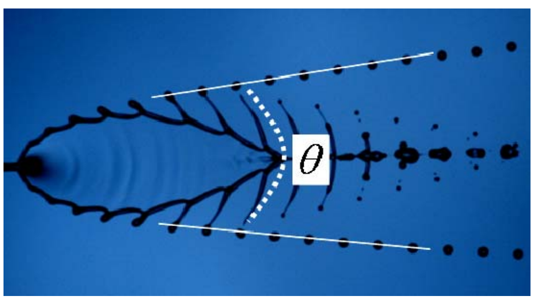

Figure 5. Definition of maximum fishbone angle (MFA)

Viscoelasticity effects on the fishbone regime

The effects of fluid viscoelasticity on the flow structure are most clearly observed in the context of the fishbone structure. As discussed above and shown in Figs. 3(b) and 4, in this regime the flow pattern consists of a single oval fluid sheet bounded by a thicker rim which becomes unstable forming ligaments and droplets. It is highly likely that the perturbation is initially triggered by the part of the fluid flowing upwards after colliding. The instability starts from the upper part of the sheet and continues to develop around the rim, ending up forming a longitudinal ligament which eventually breaks up into droplets. It is useful to introduce the concept of the 'fishbone angle' to describe the degree of development of the fishbone structure. The fishbone angle is defined as the angle formed by extending the line through the first two successive pairs of droplets on each side of the fishbone structure, as illustrated in Figs. 4(d) and 5. The maximum fishbone angle (MFA) is the angle θ when the flow structure is fully developed, just before it changes to the next regime (i.e. the smooth fluid sheet shown in Fig. 3(c)). For precise and reliable measurement through the imaging processing technique, two consecutive droplets on each set respectively were selected when they had just detached from the ligaments. The computed centers of mass of those four droplets were used to retrieve the angle defined by the four droplets.

Correlation of MFA with jetting performance

In order to study the correlation between fishbone patterns in the impinging jet experiment and jetting behavior in from a DoD printhead, the same PS solutions were jetted from a Xaar XJ125-200 printhead. The fluids were jetted at room temperature (25 °C), using the same waveform timings throughout but adjusting the piezo drive level for each fluid to achieve a target velocity of ~6 m/s at 1 mm printing distance. The details of the apparatus used in this work have been published before [12]. The maximum ligament length (MLL) was measured from an image captured when the jet had just detached from the nozzle plane. MLL is one of the most crucial parameters to determine the printability of the fluid. Many printers operate at about 1 mm stand-off distance, so that 1 mm is the maximum practical ligament length for successful printing, although a maximum length of 0.4 to 0.6 mm would typically be recommended for best print quality. Fig. 6 shows typical images of jet arrays for a dilute solution (0.01 wt% PS110 in DEP) and a solution close to the limit of printability (0.4 wt% PS110).

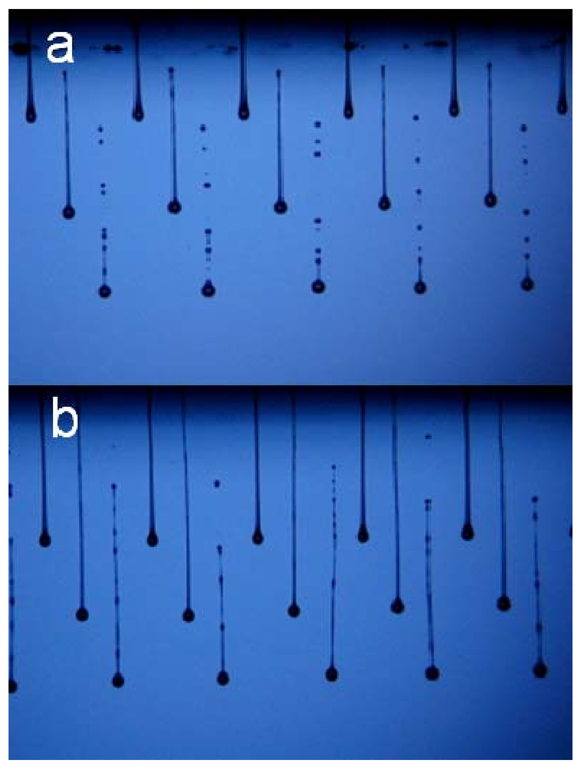

Figure 6. Images of jet arrays for a dilute polymer solution (0.01 wt% PS110) (a) and for a more concentrated solution (0.4 wt% PS110) (b).

Fig. 7 compares the values of MLL as defined above with the values of MFA for solutions of PS 110 in DEP as a function of polymer concentration. The two measurements show remarkably consistent trends. The ligament length begins to rapidly increase from 0.1 % concentration, at which MFA starts to decrease in a similar way. These effects probably occur when the solutions move from a dilute regime into a semi-dilute regime, where polymer chain-to-chain interactions start to occur. Fig. 8 shows that MFA also decreases in parallel with the increase in the elasticity ratio G'/G^*, suggesting that this is linked with the fluid elasticity. We may conclude that intermolecular interactions in these polymer solutions strongly influence the ligament length under printing conditions in the same way that they affect the fishbone structure, despite the differences in timescale and drop/ligament size.

These results suggest that the interaction of colliding continuous jets may be useful to obtain information which is relevant to the dynamics of drop formation and breakup in inkjet printing; it might for example be used to determine the maximum polymer content in fluids intended for inkjet printing. Similar results have been obtained for solutions of polystyrene with other molecular weights.

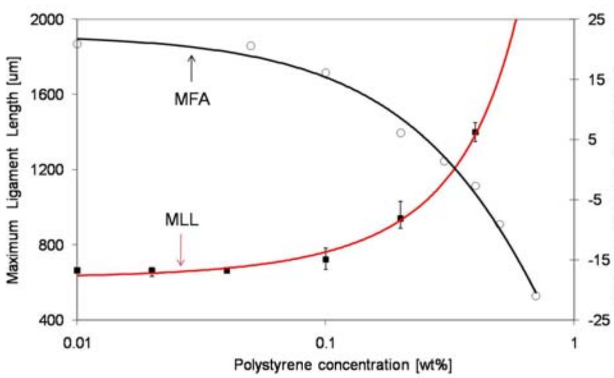

Figure 7. Comparison of the variation in maximum ligament length (MLL) and maximum fishbone angle (MFA) with polymer concentration. Both MLL and MFA begins to change rapidly above about 0.1 wt% concentration.

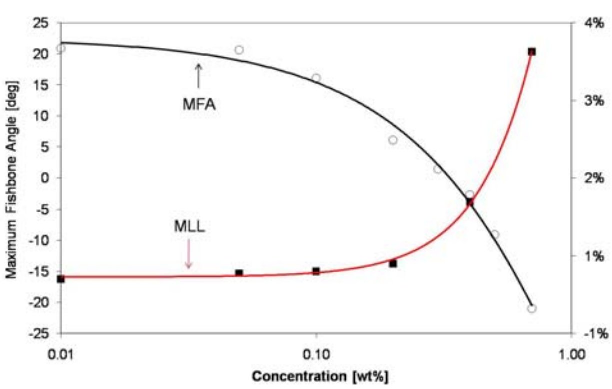

Figure 8. Comparison of maximum fishbone angle (MFA) with the elasticity ratio G'/G. All the solutions show a decrease in MFA as the elasticity ratio increases.*

Conclusions

We suggest that printability of a polymeric fluid can be predicted by observation of the symmetrical 'fishbone' structure which is generated under certain conditions by the oblique collision of two impinging jets. We have shown that fluid viscoelasticity has a strong effect on the formation and break-up of a non-Newtonian fluid sheet. As the elasticity of the fluid grows, the maximum angle defined by the fluid fishbone structure was found to decrease. Fluid fishbone patterns can be used to distinguish viscoelastic regimes in terms of degree of dilution. Good correlation is found between the maximum fishbone angle (i.e. the maximum included angle between the droplet streams in the fishbone pattern) and the maximum ligament length in jetting experiments from a DoD printhead, which suggests that the fishbone phenomenon may provide a simple and useful tool to predict the upper limit of polymer concentration in inkjet printing fluids.

References

[1] V. Subramanian, J. M. J. Frechet, P. C. Chang, et al. "Progress Toward All-Printed RFID tags: Materials, Processes, and Devices," Proc. IEEE, 93(7) (2005) 1330-1338

[2] Wen-Kai Hsiao, G. D. Martin, S. D. Hoath, I. M. Hutchings, "Ink drop deposition and spreading in inkjet-based printed circuit board fabrication," Digital Fabrication 2008 (2008) 667-670

[3] P. Calvert, "Printing Cells," Science, 318 (2007) 208-209

[4] R. H. Friend, R. W. Gymer, A. B. Holmes, et al., "Electroluminescence in conjugated polymers," Nature, 397 (1999) 121-128

[5] G. D. Martin, S. D. Hoath, I. M. Hutchings, "Inkjet printing - the physics of manipulating liquid jets and drops," J. Physics: Conference Series 105 (2008) 012001

[6] N. Reis, C. Ainsley, B. Derby, "Ink-jet delivery of particle suspensions by piezoelectric droplet ejectors," J. Applied Physics, 97 (2005) 094903

[7] D. Jang, D. Kim, J. Moon "Influence of fluid physical properties on ink-jet printability" Langmuir 25 (2009) 2629-2635

[8] T. R. Tuladhar, M. R. Mackley, "Filament stretching rheometry and break-up behaviour of low viscosity polymer solutions and inkjet fluids," J. Non-Newtonian Fluid Mechanics, 148(1-3) (2008) 97-108

[9] S. D. Hoath, I. M. Hutchings, G. D. Martin, T. R. Tuladhar, M. R. Mackley, D. Vadillo, "Links between fluid rheology and drop-on-demand jetting and printability," J. Imaging Science and Technology, 53(4) (2009) 041208

[10] J. W. M. Bush and A. E. Hasha, "On the collision of laminar jets: fluid chains and fishbones," J. Fluid Mechanics, 511 (2004) 285-310

[11] J. J. Crassous, R. Regisser, M. Ballauff, N. Willenbacher, "Characterization of the viscoelastic behaviour of complex fluids using the piezoelastic axial vibrator," J. Rheology, 49 (2005) 851-863

[12] I. M. Hutchings, G. D. Martin, S. D. Hoath, "High Speed Imaging and Analysis of Jet and Drop Formation," J. Imaging Science and Technology, 51 (2007) 438-444

Author Biography

Sungjune Jung received his M.S. in information and communication engineering in 2004 from Gwangju Institute of Science and Technology, South Korea. He then worked as an engineer at Digital Printing Division in Samsung Electronics, developing next-generation thermal inkjet print heads. Since 2007 he has been studying for a PhD at the University of Cambridge and is currently working on imaging and characterization of inkjet drop impact.